Arabian Journal for Science and Engineering (2018) 43:5295–5303
https://doi.org/10.1007/s13369-018-3158-6

RESEARCH ARTICLE - CIVIL ENGINEERING

Experimental and Numerical Analysis of Geogrid-Reinforced Soil Systems

Mabrouk Touahmia[1] · Ahmed Rouili[2] · Mustapha Boukendakdji[1] · Belkacem Achour[1]

Received: 2 March 2017 / Accepted: 12 February 2018 / Published online: 22 February 2018

Abstract
Geosynthetic-reinforced soil technique has been increasingly used in civil engineering practice over the last two decades. Understanding the response of soil reinforcements to pullout loading is considered to be essential to any successful analysis and design of reinforced soil structures. This paper presents the results of a series of experimental investigation supported by numerical analysis to examine the pullout behavior of geogrid reinforcing element under static loading. The purpose of the study is to numerically simulate the response of geosynthetic reinforcement to static pullout loading. Finite element Plaxis software was used to model the mechanical behavior of the interface between geogrid–soil dissimilar materials. The numerical model was calibrated and validated using the experimental data generated during this investigation. The results of this study demonstrate that numerical 3D model can give good predictions of the pullout behavior of geogrid-reinforced soil systems under static loads.

Keywords Soil reinforcement · Geogrid · Pullout test · Numerical modeling

1 Introduction

Geosynthetic-reinforced soil technique has been widely used in civil engineering practice over the last 20 years, and its practice is growing rapidly as infrastructure development poses an increasing demand. It has proven to offer reliable and cost-effective solutions to many soft and unstable ground problems. Various types of soil reinforcement materials have been used in many aspects of geotechnical applications such as in retaining structures, slops stability and embankment reinforcement, and in some applications, they have entirely replaced the traditional construction material. Nowadays, geosynthetic-reinforced soil technique has became a substitute solution to many unstable ground problems where the use of conventional construction techniques would be restricted or significantly expensive. The inclusion of geosynthetic materials in soil mass is known to improve soil structural capability due to the interaction resistance mobilized by the composite material. Understanding the pullout behavior of geosynthetic reinforcement is considered to be essential to any successful analysis and design of reinforced soil systems. A great deal of experimental studies have been undertaken to improve our understanding of geosynthetic-soil interaction mechanism [1–5]. Although these studies explained several interesting features of the interaction mechanism of the composite material, the design methods used for geosynthetic-reinforced soil systems have remained variable and sometimes confusing. Till now, engineers are faced with many uncertainties regarding the selection of appropriate design parameters for geosynthetic-reinforced soil systems. Up to now, the analysis and design of geosynthetic-reinforced soil systems have remained variable and sometimes confusing to many engineers. Most reinforced soil structures have been designed using limit equilibrium methods, which are generally considered to be very conservative [6–8].

In the recent decade, finite elements methods have been widely used to model the operational behavior of geosynthetic-reinforced soils and provide appropriate design specifications and guidelines for reinforced soil structures [9–12]. Numerical methods appears as an attractive approach that combines low cost and speed, allowing the evaluation of different soil-geosynthetics and boundary conditions [13].

✉ Mabrouk Touahmia
m.touahmia@uoh.edu.sa

[1] Department of Civil Engineering, College of Engineering, University of Hail, P.O. Box: 2440, Hail, Saudi Arabia

[2] Department of Civil Engineering, University of Tebessa, Tebessa, Algeria

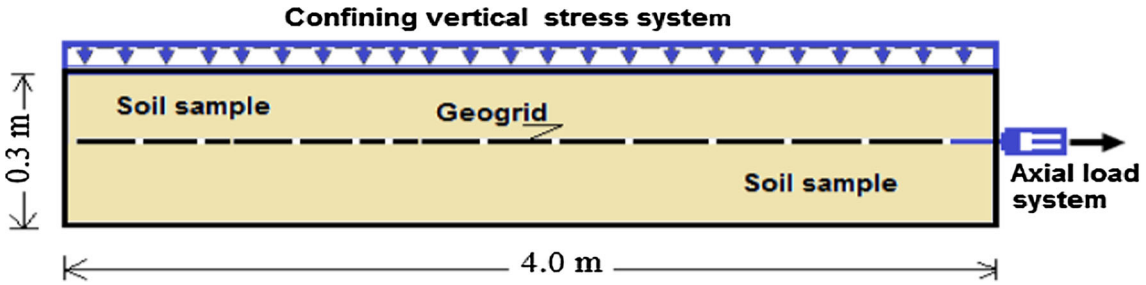

Fig. 1 Pullout test model

Several finite element codes have been developed to simulate the behavior of reinforced soil structures and model accurately their response to different loading and environmental conditions. However, the need for a numerical study that takes into consideration all main factors involved in the interaction mechanism of geosynthetic-reinforced soil systems remains essential.

This paper examines the results of pullout tests conducted on geogrid reinforcement embedded in a granular soil and subjected to static loads. The purpose of the study is to numerically simulate the response of geosynthetic reinforcement to static pullout loading. Finite element Plaxis software was used to model the mechanical behavior of the interface between geogrid–soil dissimilar materials. Some considerations about deformation behavior analysis are also analyzed.

2 Experimental Model

The testing apparatus used in this investigation is shown in Fig. 1. It consisted basically of a large-scale rigid soil container of inside dimensions 4.0 m × 0.3 m × 0.3 m, a vertical surcharge pressure setup and a pullout loading system. The pullout loads were applied to the reinforcements by adding dead weights to a load hanger located at the end of the soil container. The surcharge pressure was applied to the soil surface by means of water pressure on the top of a wooden load plate resting on the sand. The confining stress system could be controlled to 300 kN/m^2 without causing any significant straining to the experimental apparatus. The interior surfaces of the sand container were painted with aluminum coating to reduce the effect of wall friction.

The literature reveals that in most laboratory scale experiments conducted for studying the interaction behavior of soil/geosynthetic systems, small-scale models were used. This has affected the instrumentation used in the tests and has shown difficulties in exploiting the results to real structures. It was decided to use a larger near full-scale laboratory model in order to well instrument the tested reinforcements and obtain reliable measurements. The experimental device was constructed according to the recommendations of ASTM D6706-01 [14] which prescribes the standard method for measuring geosynthetic pullout resistance in soil. The pullout apparatus allows for the testing of different types of soil reinforcement materials either extensible or inextensible, a reliable evaluation of the strain distribution along the active length of the reinforcement and the application of different values of surcharge pressure on the reinforcement.

Table 1 Physical properties of SR2 geogrid

Dimensional properties	Mean
Product width (SL) (mm)	100
Transverse bar width (DTH) (mm)	12.69
Max bar thickness (DTV) (mm)	4.56
Min bar thickness (DTV) (mm)	4.36
Rib width (DLH) (mm)	5.72
Rib thickness (DLV) (mm)	1.34
Number of ribs (/m)	44
Mass per unit area (g/m^2)	972

The soil used in this investigation was a uniformly graded dry sand of medium size. A laboratory testing program performed on samples of this soil gave the following engineering properties: uniformity coefficient C_u (D_{60}/D_{10}) = 1.9; internal friction angle ϕ = 39.4°; specific gravity of solids G_s = 2.67; maximum and minimum densities = 1.78 and 1.42 Mg/m^3 respectively with corresponding void ratios of 0.491 of and 0.872. A raining method of sand placement gave an average and repeated medium bulk density of 1.59 Mg/m^3. To obtain a uniform density of soil sample, the sand was placed in equal layers of 50 mm thickness.

The reinforcement tested in this investigation was an uniaxial SR2 geogrid manufactured from co-polymer-grade high-density polyethylene. The specimen were formed by cutting the geogrid into a row of two ribs in width and 35 bars in length (approximately 4 m). The physical properties of the geogrid material is reported from manufactures' data in Table 1.

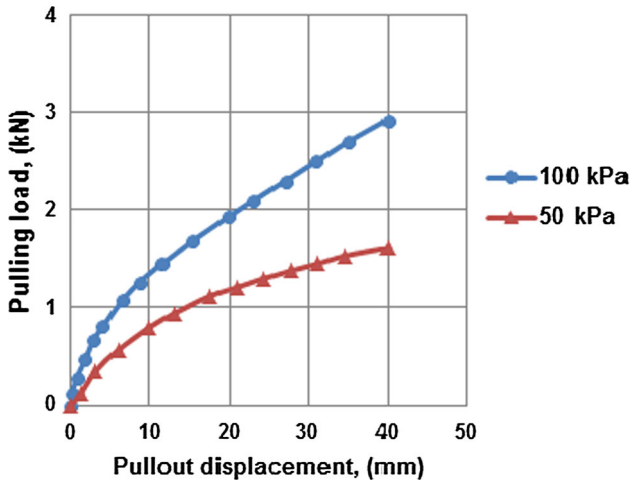

Fig. 2 Load–displacement relationships of the geogrid

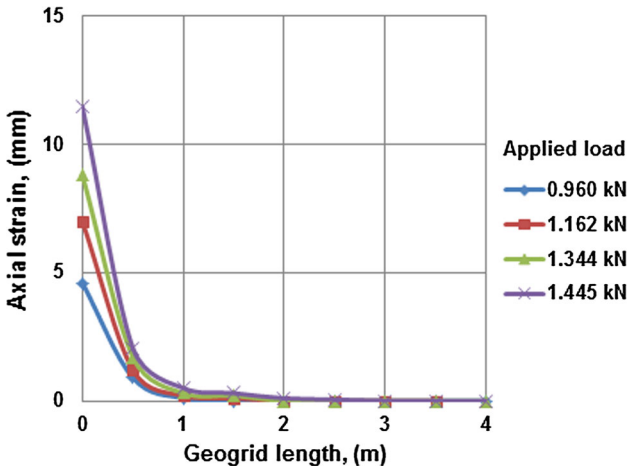

Fig. 3 Axial displacement along the geogrid

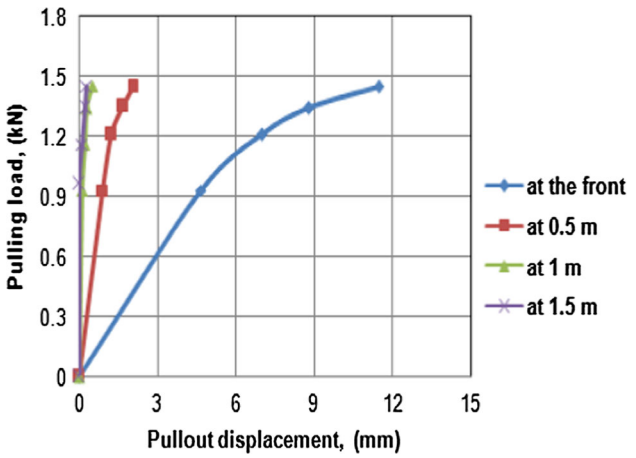

Fig. 4 Axial deformation along the geogrid at different location

3 Pullout Test Results

A series of static pullout tests were conducted on the geogrid reinforcement under two levels of normal stress (σ_n) namely 50 and 100 kPa. All tests were performed till the total pull-out displacement of the geogrid reaches a maximum of 40 mm, which represents 1% of the tested reinforcement length. Figure 2 shows the pullout displacement relationship of the geogrid reinforcement under the two fixed confining pressures. As can be seen, the general pattern of the this relationship is characterized by a continuous increase in the geogrid movement with increase in applied static pullout loads showing no total pullout failure or sudden slip. No peak load could be observed with the testing system used and the relationship between axial load and displacement became linear at higher loads. The confining pressure was found to have a significant effect on the pullout resistance of the geogrid. The reinforcement mobilized greater resistance to static pullout loads when the surcharge stress increased from 50 to 100 kPa as shown in Fig. 2. Similar conclusions have been drawn by previous researchers [15–17] in their study of the behavior of different geosynthetics under static pullout conditions and varying applied normal vertical pressure.

The recorded displacements along the geogrid length for different applied pullout loads are shown in Figs. 3 and 4. As can be seen, the total deformation of the reinforcement consists only of an extension of the front part of the reinforcement and neither slip nor extension along the rear part of the length were observed. This means that the applied pullout loads were mobilized over the front part of the reinforcement only, while the distal end remained unstrained.

and

4 Numerical Analysis

The numerical simulation was performed using the PLAXIS 3D finite elements package, in 3D parallel planes analysis with 15 nodes wedge elements. Simulation of the geosynthetic pullout test using Plaxis software is time efficient and relatively easy due to the user-friendly environment [18].

4.1 Scale Effect

The physical model described in this research was performed in a large near full-scale apparatus (container inside dimensions of 4.0 m × 0.3 m × 0.3 m) tested at 1 g. According to Bransby and Smith [19], with smooth side walls of the container and dimensions of the container used, particle size, side friction and boundary conditions do not have any significant effect on the results of the physical model. The numerical

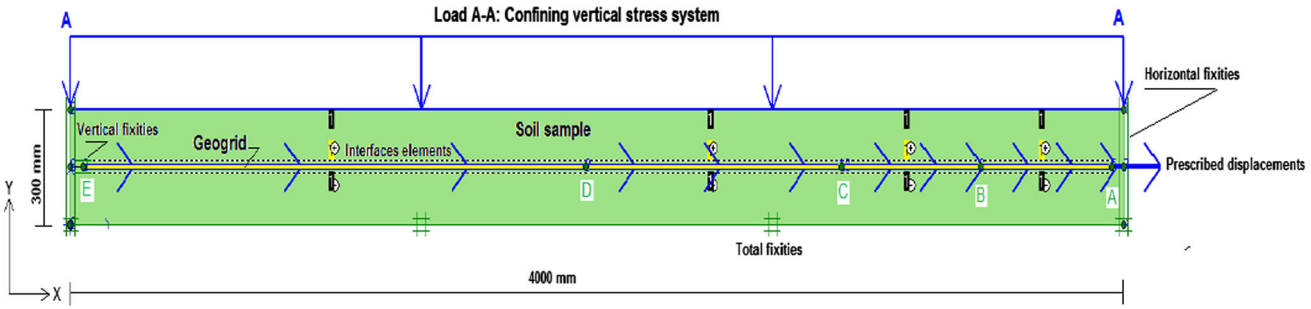

Fig. 5 General layout of the numerical model

Table 2 Soil modeling parameters

Material	γ_{unsat} (kN/m^3)	γ_{sat} (kN/m^3)	E (kN/m^2)	c (kN/m^2)	$\nu_{ur}^{(nu)}$	ϕ (^{o})	ψ (^{o})
Sand	15.6	19.7	30000	1.0	0.3	39.4	2.0

simulation was performed at full scale under 1 g (without scaling factor), taking into account the real experimental apparatus layout, the real geometry, dimensions, the boundary conditions, the loading conditions and the materials used for testing. The general layout of the model is presented in Fig. 5.

4.2 Materials Modeling and Mesh Data

The properties of the soil used in the elasto-plastic model are shown in Table 2, where γ_{unsat} and γ_{sat} are the soil unit weights; E is Young's modulus; φ and c are the soil frictional angle and cohesion, respectively; ν is Poisson ratio. The modeling mesh data adopted in the finite element computation for the soil and the interface are based on a medium coarse mesh, 15 nodes wedge elements leading to 690 elements, 3355 nodes and 4140 stress points. The reinforcement was modeled using the geogrid material option integrated in the Plaxis; the tension-only stiffness of the ribs is modeled by the axial stiffness ($EA = 0.6$ kN/mm).

4.3 Boundaries and Loading Conditions

The boundary conditions were setup manually according to the soil and geogrid displacements allowed in the experimental apparatus. Horizontal fixities were applied to each side of the vertical edges of the soil mass, and total fixities were applied to the bottom surface of the soil to simulate the contact of the soil with the experimental box. To reproduce numerically the displacement pattern of the geogrid, vertical fixities were applied to the edge's nodes (A and E) to insure the one-dimensional x-displacement of the ribs. Other nodes were defined: B, C, D on the model, corresponding to distances from the front of the rib (node A) of 500, 1000 and 2000 mm, respectively.

The confining pressure applied on the surface of the soil is simulated by a distributed load system (A–A). Prescribed one-dimensional horizontal displacements were applied to the geogrid rib at the nodal points *A, B, C, D* and *E* . To account for the interaction between the geogrid lateral surfaces and the soil, linear interface elements were defined alongside the geogrid ribs. This was proven to enhance the flexibility of the finite element meshing and prevent non-physical result [20].

During the stressing and horizontal displacements of the geogrid reinforcement, it is evident that the contact of the soil grains with the reinforcement surfaces remains permanent; therefore, interfaces elements with rigid strength apply with corresponding default value of $R_{inter} = 1$.

After defining the dimensions of the model in the (z) direction, which consist of 4 planes and 3 slices, the generated 3D numerical model is presented in Fig. 6. A partial geometry of the 3D model is presented in Fig. 7, where the upper parts of the geometry front plane, the first slice, the vertical distributed load system and the prescribed displacements applied to the ribs, are deactivated in order to show and check the real configuration and dispositions of the reinforcement ribs. In this Figure, the horizontal prescribed displacements applied to the geogrid reinforcement are activated. As mentioned previously, the experimental results show that the distribution of displacements along the geogrid length is not constant. The total displacement consisted only of an extension of the front part of the reinforcement, and neither slip nor extension along the half rear segment of the geogrid length were observed . To numerically simulate this finding, 4 levels of prescribed displacements are applied to the geogrid frontal nodal point (A), then, different prescribed displacements multipliers are applied to the nodal points (*B, C, D* and *E*) as shown in Table 3. These values are estimated on the basis of the experimentally observed extension of the geogrid.

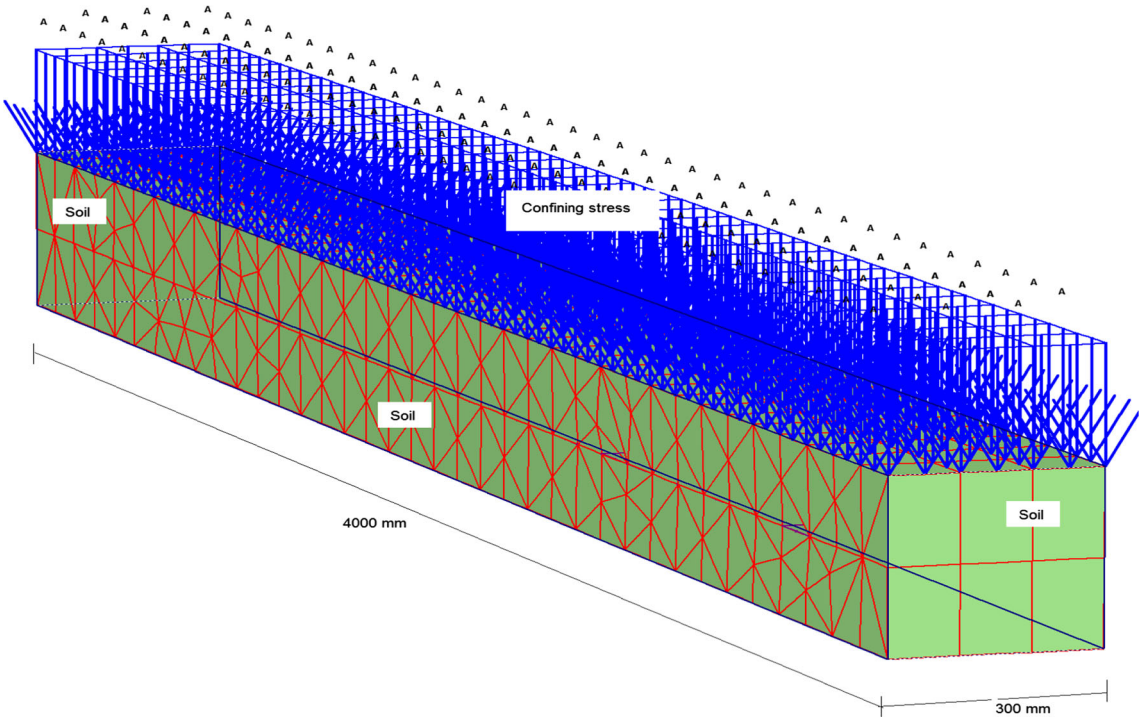

Fig. 6 Typical 3D finite elements model

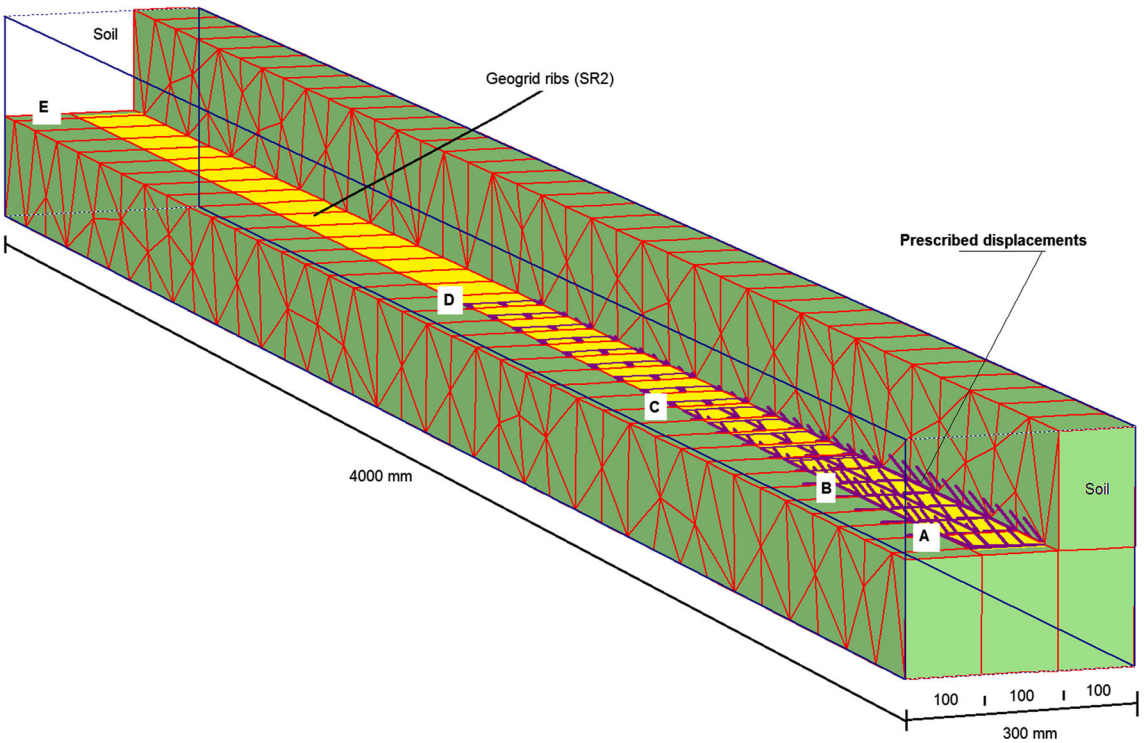

Fig. 7 Partial geometry of the 3D model with applied prescribed displacements

Table 3 Prescribed displacements of the geogrid

Nodes	Distance from A (mm)	Multipliers	Prescribed displacements (mm)			
A	0					
		1.0	10	20	30	40
B	500					
		0.4	4	8	12	16
C	1000					
		0.2	2	4	6	8
D	2000					
		0	0	0	0	0
E	4000					

4.4 Calculation Types and Phases

To account for the testing procedure and to replicate numerically as close as possible the experimental testing procedure, the calculation process was run in fives phases, taking into account the initial conditions applied in the experimental work. The first calculation phase consist of a 3D Plastic calculation with a staged construction loading input. In this phase, the geometry of the model is defined (by activating and deactivating soil clusters and the geogrids element in different planes and slices (following the z axis) in order to simulate in 3D the real configuration of the model. At this stage, the loading parameters (distributed load system A–A) is applied and the prescribed displacements applied to the reinforcement are deactivated. The loading procedure of the geogrid reinforcement is then applied in 4 steps through the activation of the horizontal prescribed displacements systems, 3D plastic calculation with total multiplier loading input were applied, resulting in 4 calculations phases. For each phases after fully reaching the prescribed ultimate state, the values of the horizontal forces (pulling load) is computed.

4.5 Numerical Results

4.5.1 Deformed Mesh

Typical deformed mesh of the 3D model (with partial geometry) is presented in Fig. 8, corresponding to the final phase (5) output. As shown, it is clear that the model is simulating the observed experimental displacements of the geogrid reinforcing element within the soil mass. It can be seen that the prescribed horizontal displacements of the geogrid imposed in this calculation phase (40 mm) is well simulated by the model which indicates good quality of the numerical analysis.

4.5.2 Stresses in the Soil Mass (Plastic Points)

In the present analysis, the soil was modeled by the Mohr–Coulomb model. The variation of the total stress condition in the model is presented in Figs. 9a, b with partial geometry effect, where the distribution of the plastic points (red-squares) corresponding to the initial phase (1) and the final loading phase (5) are presented. A plastic point or plastic failure point is a point which is currently on the Mohr–Coulomb envelope (function of the cohesion and the friction angle of the soil), which corresponds to an irreversible plastic stress state in the numerical model. From Fig. 9, it is evident that the increase in the stresses states in the model and the prescribed displacements of the reinforcement causes relative development of failure points within the soil mass and around the reinforcement element. As expected, the plastic states in the soil are function of the applied confining stress and the prescribed displacements imposed to the geogrid reinforcement. It could also be noticed that the dimensions of the experimental box (and consequently the dimension of the model) are well defined as the interaction of the soil with the box boundaries have little effect on the results.

4.5.3 Displacements of the Geogrid Reinforcement

The displacements of the geogrid are checked out by means of the calculation of the horizontal displacements of some carefully selected nodes (A and B), corresponding to the physical length limit of the geogrid ribs (the selected nodes are indicated in Fig. 7). The computed horizontal displacements (U_x) of the nodes (A and B) for a confining stress of 100 kPa are plotted against the horizontal force (F_x) simulating the axial pulling load (Fig. 10). It can be seen that the computed displacements of the geogrid consists only of an extension of the front part of the reinforcement and no deformation along the rear part of the geogrid takes place. This result is in good agreement with the experimental data which showed that displacements occur only over the front

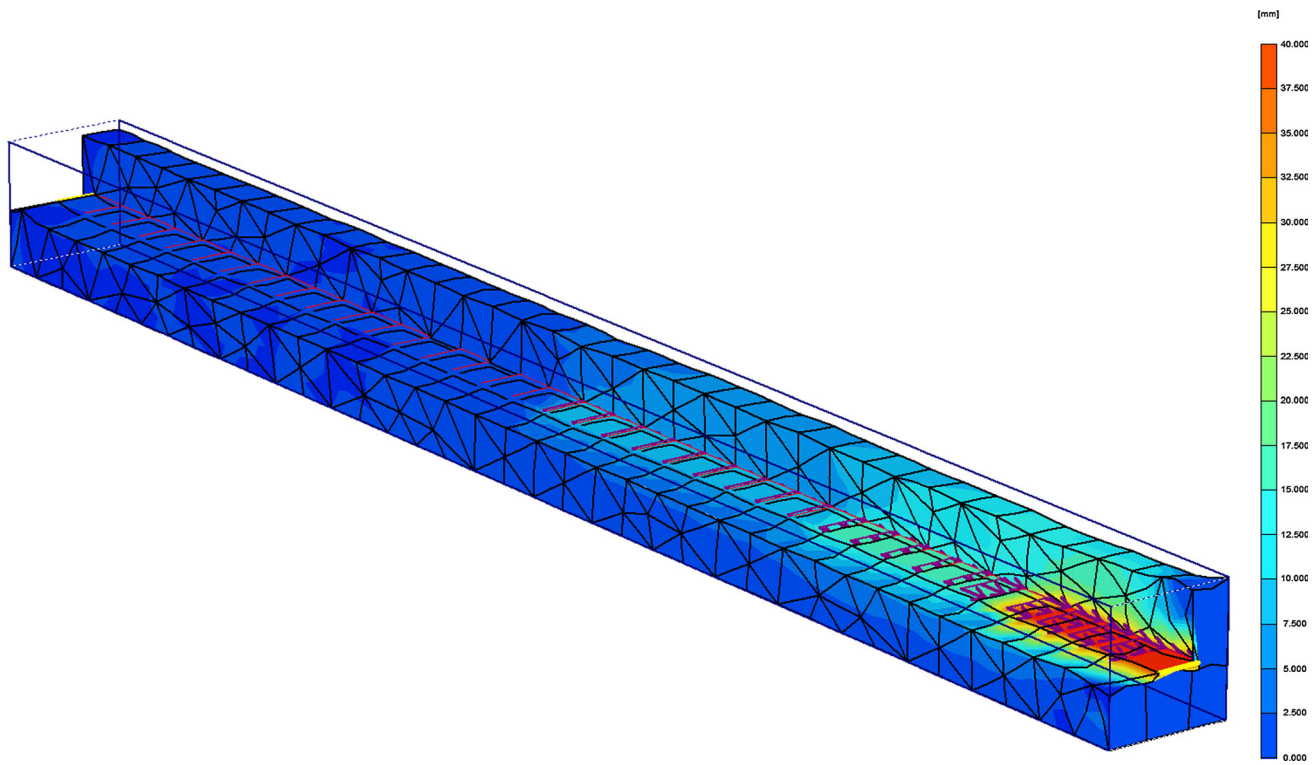

Fig. 8 Deformed mesh-horizontal displacements for the phase 5

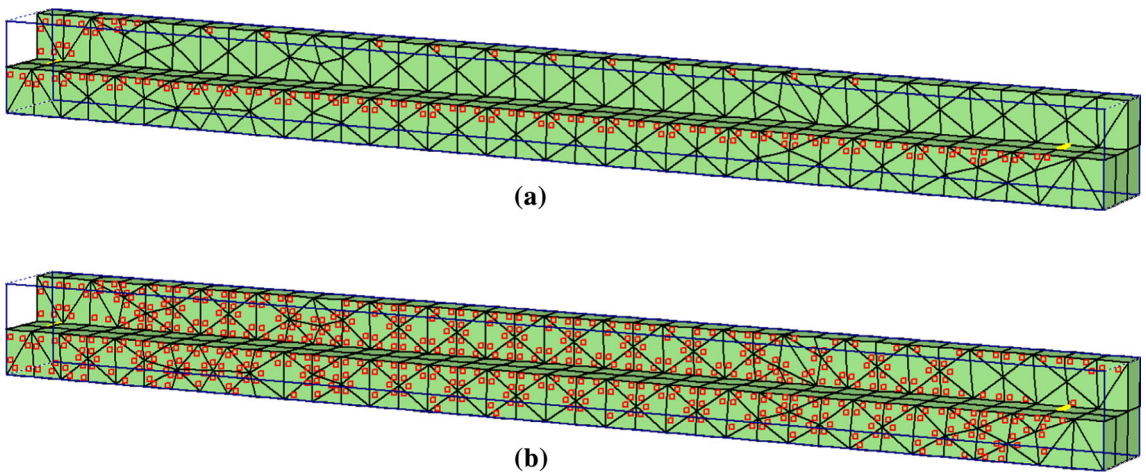

Fig. 9 **a** Plastic points in the model Phase 1 (without pulling load). **b** Plastic points in the model Phase 5 (prescribed displacement of 40 mm)

half of the reinforcement length (Fig. 3), the parts toward the distal end remain unstrained.

4.5.4 Validation of the Model

In Fig. 11, the computed displacements of the geogrid reinforcement are plotted against the corresponding measured and numerically computed pulling loads. Two sets of results are presented, corresponding to confining stresses of 50 and 100 kPa. As for the experimental results, the predicted displacement of the geogrid shows no peak load and the relationship between load and deformation tends to became linear at larger displacements.

It is interesting to note that the computed load–displacement relationships are in good agreement with measured results. The small discrepancy between the measured and numerically computed results could be attributed to many factors; including numerical computation errors (3–5%), the rheological soil model, the modeling of the soil-reinforcement interaction. However, it could be stated that the proposed

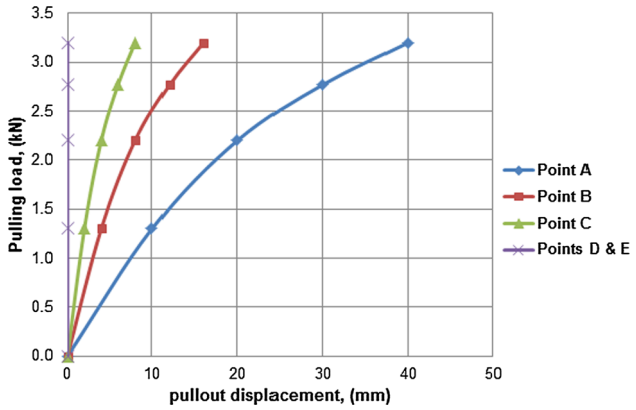

Fig. 10 Computed axial deformation along the geogrid

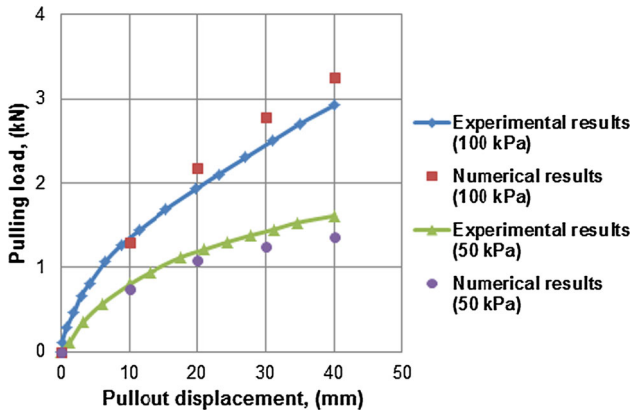

Fig. 11 Numerical and experimental load–displacement relationships of the geogrid

numerical 3D model is capable of predicting the load carrying capacity and the subsequent displacements of the geogrid reinforcement with a high level of accuracy. This approach could be relevant for design practice in estimating numerically the pullout load limits to be imposed to avoid uncontrolled extension of geogrid reinforcements leading to failure of soil-reinforcement structures.

5 Conclusions

This study investigated the pullout performance of geogrid soil reinforcement under different confining vertical pressures. A series of laboratory tests supported by numerical analysis were conducted on geogrid element embedded in a uniformly graded dry sand of medium density. The experimental results provided a better understanding of the interaction mechanism and failure mode of soil–geogrid composite material. Finite element Plaxis software was used to model the mechanical behavior of the interface between geogrid–soil dissimilar materials. The developed numerical model was calibrated and validated using the experimental data generated during this investigation. The study brings the following conclusions for geogrid reinforcement:

- The experimental results showed that load–displacement relationship of the geogrid reinforcement was characterized by a continuous increase in movement with increase in applied loads showing no total pullout failure.
- The pullout behavior of geosynthetic-reinforced soil systems can be simulated by numerical methods. The numerical analysis using Plaxis software has shown good predictions of the pullout response of geosynthetic-reinforced soil systems.
- The proposed numerical 3D model is in good agreement with the measured values obtained for the load carrying capacity of the geogrid reinforcement. This approach could be relevant for design practices in estimating numerically the pullout load limits to be imposed to avoid uncontrolled extension of geogrid reinforcements leading to failure of soil-reinforcement structures.

Acknowledgements The research reported herein was funded by the Deanship of Scientific Research at the University of Hail, Saudi Arabia. The authors would like to express their sincere gratitude to the Deanship of Scientific Research and to the College of Engineering at the University of Hail for providing all facilitations required for this research.

References

1. McGown, A.: The behavior of geosynthetic reinforced soil systems in various geotechnical applications. In: Proceedings of the 2nd European Conference on Geosynthetics EuroGeo2000, Bologna, Italy, vol. 1, pp. 3–26 (2000)
2. Palmeira, E.M.: Soil-geosynthetic interaction: modeling and analysis. Geotext. Geomembr. **27**(5), 368–390 (2009)
3. Hossain, M.B.; Hossain, M.Z.; Sakai, T.: Interaction properties of geosynthetic with different backfill soils. Int. J. Geosci. **3**(5), 1033–1039 (2012)
4. Giroud, J.P.: Quantification of geosynthetic behavior. Geosynth. Int. **12**(1), 2–27 (2015)
5. Pinho-Lopes, M.P.; Paula, A.M.; Lopes, M.L.: Soil-geosynthetic interaction in pullout and inclined-plane shear for two geosynthetics exhumed after installation damage. Geosynth. Int. **23**(5), 331–347 (2016)
6. Zornberg, J.G.; and Leshchinsky, D.: Comparison of international design criteria for geosynthetic reinforced soil structures. In: Ochiai et al. (eds.) Landmarks in Earth Reinforcement, vol. 2, pp. 1095–1106 (2003)
7. Leshchinsky, D.: On global equilibrium in design of geosynthetic reinforced wall. J. Geotech. Geoenviron. Eng. ASCE **135**(3), 309–315 (2009)
8. Yang, K.H.; Utomo, P.; Liu, T.L.: Evaluation of force-equilibrium and deformation based design approaches for predicting reinforcement loads within geosynthetic reinforced soil structures. J. GeoEng. **8**(2), 41–54 (2013)
9. Perkins, S.W.; Edens, M.Q.: Finite element modeling of a geosynthetic pullout test. Geotech. Geol. Eng. **21**, 357–375 (2003)

10. Hatami, K.; Bathurst, R.J.: Numerical model for reinforced soil segmental walls under surcharge loading. Can. Geotech. J. **67**(4), 1066–1085 (2006)
11. Bergado, D.T.; Teerawattanasuk, C.: 2D and 3D numerical simulations of reinforced embankments on soft ground. Geotext. Geomembr. **26**(1), 39–55 (2008)
12. Yu, Y.; Damians, I.P.; Bathurst, R.J.: Influence of choice of FLAC and PLAXIS interface models on reinforced soil–structure interactions. Comput. Geotech. **65**, 164–174 (2015)
13. Sieira, A.C.F.: Pullout behavior of geotextiles: numerical prediction. Int. J. Eng. Res. Appl. **6**(11–4), 15–18 (2016)
14. ASTM Standard D6706-01: Standard Test Method for Measuring Geosynthetic Pullout Resistance. ASTM International, West Conshohocken (2007)
15. Moraci, N.; and Cardile, G.: Pullout behaviour of different geosynthetics embedded in granular soils. In: Proceedings of the 4th Conference on Geosynthetics. Changhai, China, pp. 146–150 (2008)
16. Bolt, A.F.; and Duszynska, A.: Pull-out testing of geogrid reinforcements. In: Proceedings of the 2nd European Conference on Geosynthetics. EuroGeo2000, Bologna, Italy, vol. 1 (2000)
17. Teixeira, S.H.C.; Bueno, B.S.; Zornberg, J.G.: Pullout resistance of individual longitudinal and transverse geogrid ribs. J. Geotech. Geoenviron. Eng. **133**(1), 37–50 (2007)
18. PLAXIS: Plaxis Materials Model Manual. Delft, The Netherlands. Plaxis bv (2011)
19. Bransby P.L.; and Smith, I.A.A.: Side friction in model retaining wall experiments. J. Geotech. Eng. ASCE, GT7, pp. 615–632 (1975)
20. Langen, H.V.; Vermeer, P.A.: Interface elements for singular plasticity points. Int. J. Numer. Anal. Methods Geomech. **15**(5), 301–315 (1991)